Further results on multifractality in shell models

D. Pisarenko
CNRS, Observatoire de Nice, B. P. 229, 06304 Nice Cedex 4, France and MITPAN, 79/2 Warshavskoye sh., 113556 Moscow, Russia

L. Biferale
CNRS, Observatoire de Nice, B. P. 229, 06304 Nice Cedex 4, France and Dipartimento Fisica, Università di Roma, "Tor Vergata," Italy

D. Courvoisier and U. Frisch
CNRS, Observatoire de Nice, B. P. 229, 06304 Nice Cedex 4, France

M. Vergassola
CNRS, Observatoire de Nice, B. P. 229, 06304 Nice Cedex 4, France and Dipartimento Fisica, Università di Roma, "La Sapienza," Italy

(Received 4 January 1993; accepted 14 May 1993)

Very long integrations, involving hundreds of millions of time steps, have been performed for the Gledzer–Ohkitana–Yamada "shell model" of fully developed turbulence, thereby allowing the computation of essentially noise-free structure functions at all inertial- and dissipation-range scales. Previously reported results by Jensen *et al.* [Phys. Rev. A **43**, 798 (1991)] on the multifractal behavior of this model are confirmed. Oscillations in the structure functions are found to be genuine. An exact relation for certain cubic moments, equivalent to Kolmogorov's four-fifth law, is derived and tested. The third-order structure function, here defined in terms of the third moment of shell amplitudes, is not directly determined by this relation and need not have its exponent equal to one. Significant discrepancies are actually found when the ratio between successive shell wave numbers is less than two.

I. INTRODUCTION

Kolmogorov's 1941 (K41) theory of fully developed turbulence predicts that the structure function of order p, i.e., the pth order moment of the velocity increment, scales with an exponent $p/3$ over inertial-range separations. Discrepancies for $p=2$, which are sometimes reported, are usually considered too small to be significant. Measurements of *high*-order structure functions are rather difficult. Indeed, by definition, they require accurate measurements of high-order moments of velocity increments. The latter involve the tail of the corresponding probability distribution functions, corresponding to very rare events. Hence, it is necessary to process very long records of the turbulent signal. Early measurements of structure functions were limited by recording capabilities. As shown by Anselmet *et al.* this can lead to vastly overestimating the discrepancy between the measured exponents and their K41 predictions.[1] Also, high-order structure functions are not well represented by pure power laws, as evidence, for example, by Fig. 13 of Ref. 1. Still, Anselmet *et al.* do present a good case for the existence of discrepancies from K41.

From a theoretical viewpoint, intermittency may be seen as a breaking of (statistical) scale invariance due to the presence of an external scale. Intermittency is ruled out in closure models, which are generally constructed in such a way that K41 is an exact stable solution at small scales, unaffected by the external scale. Stability in closure models is intimately related to the fact that the dynamical variables are averaged quantities. A very interesting class of "toy models" for turbulence, in which chaotic fluctuations and intermittency are not *a priori* ruled out are the *shell models* which originated with the Russian school in the seventies (see Refs. 2, 3–6, and references therein). Shell models are constructed by retaining only the slimmest contact with the Navier–Stokes equations, viz. the deterministic and quadratic character of the equations, energy conservation, and scale invariance. Shell models may also be viewed as severe truncations of the Navier–Stokes equations, retaining only one real or complex mode u_n as a representative of all the Fourier modes in the shell of wave numbers k between $k_n=k_0q^n$ and k_{n+1} (an octave in the simplest case of $q=2$). In order to mimic the supposed "local" (in scale) character of nonlinear interactions, only couplings to the nearest or next nearest shells are kept. In this paper we shall be interested in the Gledzer–Ohkitani–Yamada (GOY) model which is governed by the following set of complex coupled ODE's:

$$\left(\frac{d}{dt}+\nu k_n^2\right)u_n=i(a_nu_{n+1}u_{n+2}+b_nu_{n-1}u_{n+1}+c_nu_{n-1}u_{n-2})^*+f_n, \tag{1}$$

where $*$ stands for complex conjugation. Although, this model is sometimes referred to as the Ohkitani–Yamada model, these authors have pointed out in Ref. 4 that "... it may be considered as a complex version of Gledzer's[2] model." Hence, the name here proposed. Most of the missing details in the definition of the model will be given in the next section. Let us just stress that in the shell models, the moments of order p of the absolute value of u_n and the wave number $k_2=k_0q^n$ are used in lieu of the structure

 0899-8213/93/5(10)/2533/6/$6.00

functions and the inverse of the spatial increment, respectively. Averages are computed over time and/or over ensembles of random initial conditions.

Jensen *et al.*[6] have reported high-Reynolds number integrations of the GOY model (for $q=2$) which reveal departures from K41: the structure function of order p varies as $k_n^{-\zeta_p}$ in the inertial range and the graph of ζ_p vs p drops significantly below the K41 value $p/3$ for $p \geqslant 5$. Furthermore, the graph displays curvature, an indication of multifractality.[7] The aforementioned difficulties, encountered in the determination of the scaling exponents ζ_p from experimental data, are also present in the case of numerically simulated shell models. Such issues were not in the focus of the studies reported in Ref. 6. One of our goals is to repeat the calculations for GOY model, while carefully examining the question of error bars for scaling exponents. In the next section, we present our numerical results, which are substantially confirming those of Ref. 6 and make several new observations. Section III is devoted to the generalization of Kolmogorov's four-fifth law for the third-order structure function.

II. NUMERICAL SIMULATIONS: STRUCTURE FUNCTIONS AND SCALING EXPONENTS

Before describing our numerical implementation, we give a few more details concerning the GOY model, governed by (1). The "shell index" n runs from one to infinity. All u_n's with $n \leqslant 0$ are taken to be zero. The coefficients, chosen to ensure energy conservation, are given by

$$a_n = k_n = k_0 q^n, \quad b_n = -\frac{1}{2} k_{n-1}, \quad c_n = -\frac{1}{2} k_{n-2}, \tag{2}$$

where k_0 is a reference wave number and q is the aspect ratio (ratio between successive shell wave numbers). Unless otherwise specified, we take $k_0 = 2^{-4}$ and $q=2$ (octave shells), as in Ref. 6. The "forcing," restricted to the fourth shell, is given by

$$f_n = \delta_{4,n}(1+i) \times 5 \times 10^{-3}. \tag{3}$$

In the numerical implementation, the model is truncated to a finite number of shells, with n running from 1 to $N=22$ and $u_n = 0$ for $n > N$. Temporal discretization uses a (second-order) slaved Adams–Bashforth scheme, viz.

$$u_n(t+\delta t) = e^{-\nu k_n^2 \delta t} u_n(t) + \frac{1-e^{-\nu k_n^2 \delta t}}{\nu k_n^2} \times \left(\frac{3}{2} g_n(t) - \frac{1}{2} g_n(t-\delta t) \right), \tag{4}$$

where $g_n(t)$ stands for the right-hand side of (1). This scheme is a variant of the "slaved frog" scheme of Ref. 8. Such slaved schemes take advantage of the very fast damping of high wave-number modes. At the initial time t_0, the same scheme is used with $g_n(t_0 - \delta t) = g_n(t_0)$, which is only first order accurate, an irrelevant point in the context of the present study. In all runs reported in this section, the viscosity has the value $\nu = 10^{-7}$, which ensures a well-resolved dissipation range (see below). The time step is $\delta t = 10^{-4}$, small enough to ensure stability of integration. Initial conditions (communicated to us by K. Ohkitani and M. Yamada) were chosen "on the attractor," i.e., from the output of a preliminary very long run with the same parameters. (This was also used for debugging purposes.) The total number of time steps is 250×10^6. This corresponds roughly to five thousand turnover times at the forcing scale and to a million turnover times at the high wave-number end of the inertial range. Note that the inverse of the square root of these numbers gives a measure of the relative noise in time-averaged statistical quantities.

The moduli of the u_n's are stored at each time step and time averages are then computed over the whole run or fractions thereof. Such operations must be performed in double precision (64 bits) to avoid roundoff problems in summing huge numbers of data. Most computations were performed on a SONY 3410 workstation and took about 15 min of CPU per million time steps (including postprocessing). The main quantities of interest are the structure functions, here defined as

$$S_p(n) = \langle |u_n|^p \rangle. \tag{5}$$

Figures 1(a) and 1(b) are plots of the computed structure functions for $p=2, 3, \ldots, 10$ (from top to bottom). The horizontal scale is linear in the shell index and the vertical is logarithmical, so that powers laws $k_n^{-\zeta_p}$ can be identified from the slope of the graph. Figure 1(a) shows the averages after the first 20×10^6 time steps, while Fig. 1(b) is after 250×10^6 time steps (in identical scales). Superposing the figures, very significant discrepancies are observed at wave numbers less or equal to the forcing wave number. At inertial-range scales, i.e., those scales where the structure functions follow power laws, there are still significant discrepancies for large orders. But comparisons of outputs after 150×10^6 (not shown) with those of Fig. 1(b), indicate that, over the entire inertial range and the part of the dissipation range shown, structure functions are essentially noise-free beyond 150×10^6 time steps. The discrepancies at the very smallest wave numbers (to the left of the forcing wave number) are easily explained by noting that the corresponding turnover times are so large that longer time averaging would be required (if one cared).

Let us now comment on various features observed in the plots of structure functions. The wave number where the structure functions appear to bend over into a dissipation range shows a marked shift to the right (higher wave numbers) as the order p increases. This is in qualitative agreement with predictions of the multifractal model. Indeed, according to Refs. 9 and 10 the viscous cutoff scales as $\nu^{1/(1+h)}$, where h is the multifractal scaling exponent which minimizes $ph + 3 - D(h)$, a decreasing function of p. Still, multifractal phenomenology does not predict the variation with p of the dimensionless constants in such scaling laws, so that predicting how the viscous cutoff changes with p at fixed ν is delicate. In spite of the increase of the dissipation wave number with the order, all the structure functions shown here have a clean dissipation range. [This is not the case for the twelfth-order structure function shown in Fig. 1(b) of Ref. 6.]

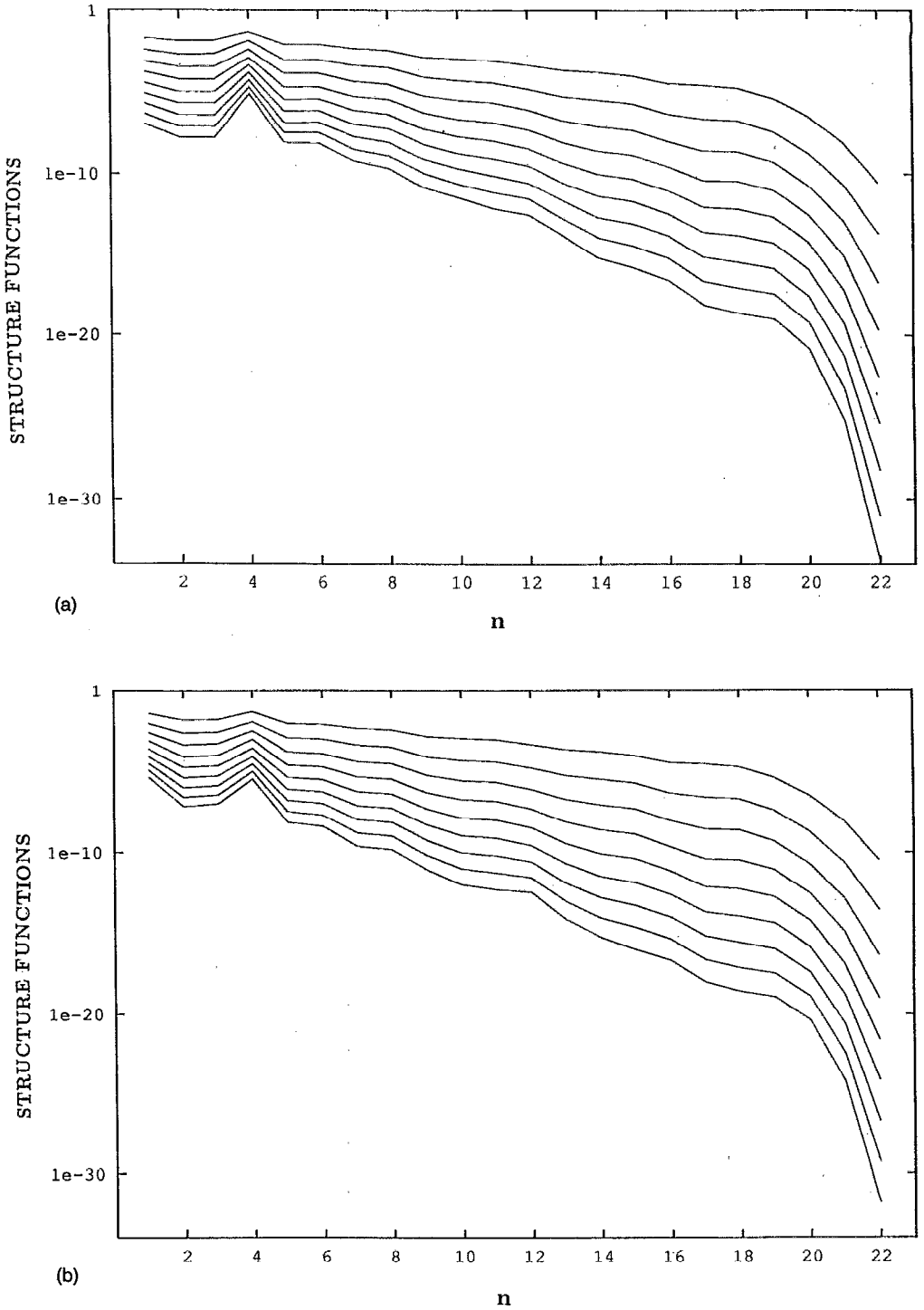

FIG. 1. Structure functions of order two through ten (top to bottom) for the Gledzer–Ohkitani–Yamada model. The shell index n is $\log_2$ of the wave number. The data are averaged over (a) 20×10^6 time steps and (b) 250×10^6 time steps. Notice the shift to high wave numbers of the viscous cutoff as the order increases.

The substantial range of scales (about 11 octaves) over which the structure functions follow (noise-free) power laws allows a quite accurate determination of the exponents ζ_p. This is done by a linear least-square fit of $\log_2 S_p(n)$ to a straight line of slope $-\zeta_p$. The fit is done in an interval $(n_{\min},n_{\max})$ which may be determined either visually or, here, by minimizing the fit error. The values $n_{\min}$ and $n_{\max}$ depend slightly on p, a good tradeoff being $n_{\min}=6$ and $n_{\max}=18$. Figure 2 shows a plot of ζ_p vs p together with the error bars generated in the fit. The computation used all 250×10^6 time steps. The dashed line corresponds to K41: $\zeta_p=p/3$.

It is immediately seen that the data are not at all consistent with K41 for $p\geqslant6$, and only marginally consistent for $p=2,3,5$. (The issue of discrepancies for $p=3$ will be discussed separately in Sec. III.) Furthermore, no straight

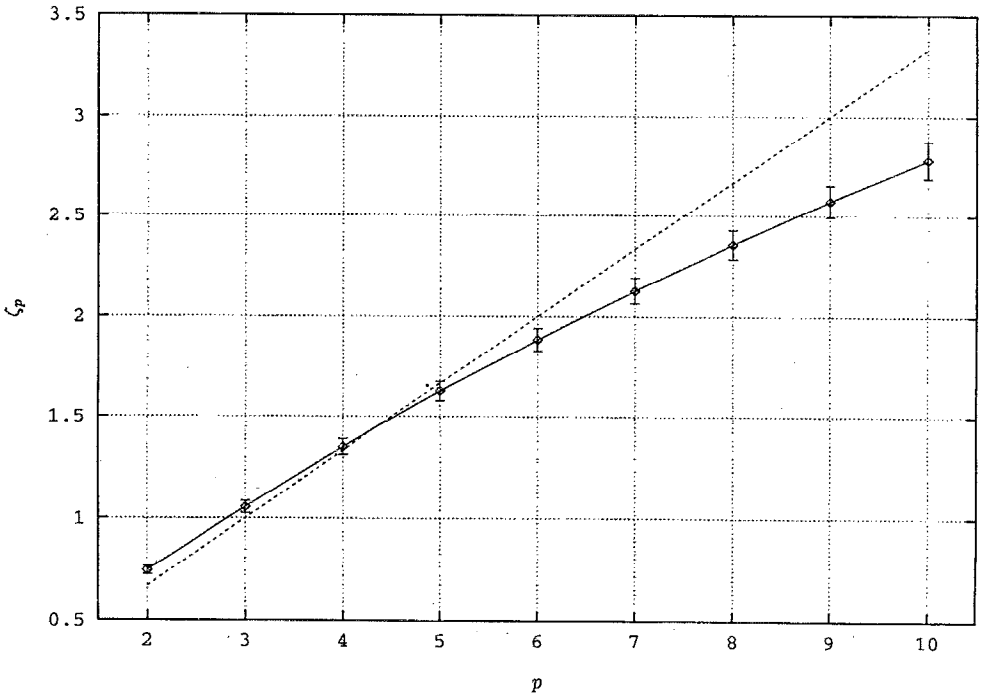

FIG. 2. Scaling exponent ζ_p for the structure function vs order p. The dashed line corresponds to K41 ($\zeta_p=p/3$). The error bars are from a least-square fit of the structure functions shown in Fig. 1(b) to a power law in the interval $6\leqslant n\leqslant 18$.

line (as assumed by the β model) can be drawn through the data points, so that *multifractality* of the GOY model is here given further support. Recently an analytic method giving ζ_p for the GOY model has been proposed in Ref. 11. It involves some heuristic steps but has no continuously adjustable parameters and gives values within our error bars.

One of the major causes of errors in the ζ_p's are the *oscillations* seen in the structure functions at inertial-range scales. There is no doubt that they are genuine. Indeed, our results have recently been reproduced by Léveque, using a different numerical scheme and averaging over one thousand systems running in parallel for 10^6 time steps.[12] We note that oscillatory deviations from pure power-law behavior in experimental results of the sort reported in Ref. 1 have been interpreted as reflecting the lacunarity of fractal sets by Smith *et al.*[13]

III. SCALING PROPERTIES OF THIRD-ORDER MOMENTS

In his third 1941 turbulence paper, Kolmogorov established an exact relation for the third-order longitudinal structure function which, in the limit of vanishing viscosity, reads

$$\langle[\delta v(l)]^3\rangle=-\frac{4}{5}\epsilon l, \tag{6}$$

where ϵ is the mean rate of energy dissipation (assumed to stay finite and positive in the limit $\nu\to 0$) and l is the separation. It follows from this "four-fifth" relation that the exponent for the third-order structure function $\zeta_3=1$.

For all energy-conserving shell models there is an analogous relation, which we now derive for the GOY model. Multiplying the nth equation in (1) by u_n^*, summing from $n=1$ to $n=M\geqslant 4$, adding the complex conjugate and averaging, we obtain after easy algebra

$$\left(\frac{d}{dt}\right)\sum_{n=1}^{M}\left\langle\frac{|u_n|^2}{2}\right\rangle+\nu\sum_{n=1}^{M}k_n^2\langle|u_n|^2\rangle=-\Pi_M+\epsilon, \tag{7}$$

where

$$\Pi_M=-Im\left\langle\frac{k_M}{4}(u_{M-1}u_Mu_{M+1}+4u_Mu_{M+1}u_{M+2})\right\rangle \tag{8}$$

is the (mean) energy flux through the Mth shell and

$$\epsilon=\mathrm{Re}\langle f_4u_4^*\rangle \tag{9}$$

is the (mean) energy input from the force (here restricted to the fourth shell). Let us now assume a statistical steady state in the limit of vanishing viscosity, such that the mean energy input (also the mean energy dissipation) remains finite. The left-hand side of (7) vanishes and we obtain an identity for third-order moments, viz.

$$\Pi_M=\epsilon. \tag{10}$$

A consequence of (10) is that the particular third-order quantity

$$\frac{\Pi_n}{k_n}=\mathrm{Im}\left\langle\frac{1}{4}(u_{n-1}u_nu_{n+1}+4u_nu_{n+1}u_{n+2})\right\rangle \tag{11}$$

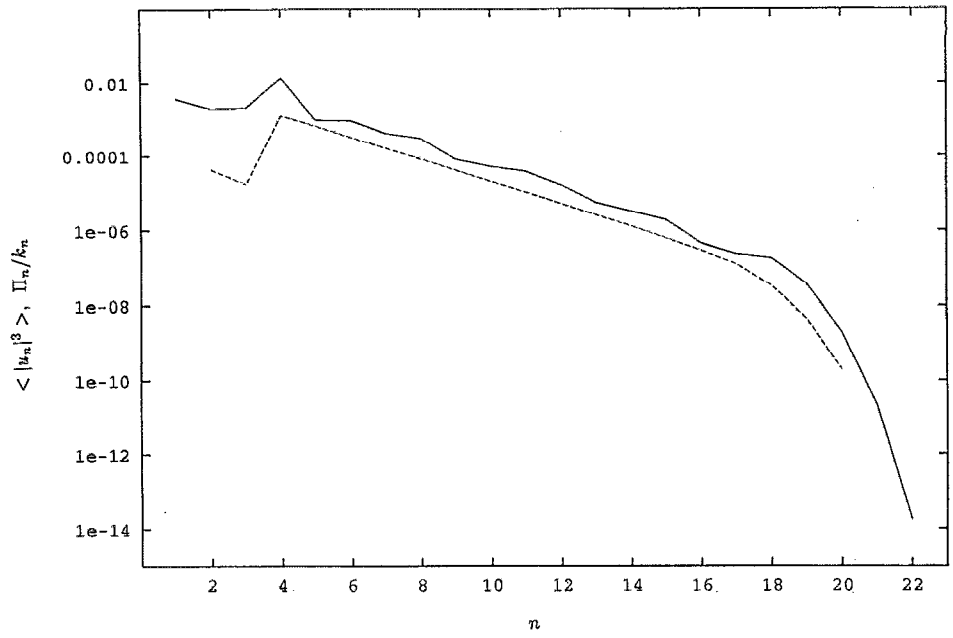

FIG. 3. Third-order structure function replotted from Fig. 1(b) (continuous line) and combinations of third-order moments involved in the energy flux Π_n (dashed line). The perfect scaling observed for the latter at inertial range scales is a check of Eq. (10), the analog of Kolmogorov's four-fifth law.

scales as k_n^{-1}, that is with the exponent $\zeta_3=1$. The quantity Π_n/k_n is however not exactly the standard third-order moment $\langle|u_n|^3\rangle$ which was calculated in Sec. II and was found to scale with an exponent ζ_3 very close to one (see Fig. 2). In Fig. 3 we replot the third-order structure function together with Π_n/k_n, the latter being now evaluated from the same simulation. We notice that the graph of Π_n/k_n is absolutely straight in the inertial range (as already observed in Ref. 4) and has exactly the scaling exponent $\tilde{\zeta}_3=1$. A similar plot (of Π_n rather than Π_n/k_n) may be found in Fig. 2 of Ref. 5. The discrepancy between the scaling exponents ζ_3 and $\tilde{\zeta}_3$ is here very slight.

We now take advantage of some freedom in the definition of the GOY model, to demonstrate that the discrepancy reported here is genuine. So far, we assumed that the GOY model had a ratio $q=2$ between successive shell wave numbers. The GOY model with $q\neq 2$ has the same energy-conservation relation as for $q=2$ and, therefore, has an expression of the energy flux, similar to (8). We have performed numerical integrations of the GOY model (1) for various values of q and determined each time the third-order structure function $S_3(n)$. Specifically, we now give results for

$$q=1.5, \quad N=31, \quad k_0=2^{-4},$$

$$f_n=\delta_{4,n}(1+i)\times 5\times 10^{-3}, \quad \nu=10^{-6}, \tag{12}$$

and for

$$q=2.5, \quad N=20, \quad k_0=2^{-4}/(2.5)^2,$$

$$f_n=\delta_{4,n}(1+i)\times 5\times 10^{-3}, \quad \nu=10^{-8}. \tag{13}$$

In both instances, we collect statistics for about five-hundred eddy-turnover times calculated at the forcing scale. In order to bring out possible deviations from the "standard" scaling $S_3(n)\propto k_n^{-1}$, we plot in Fig. 4 the quantity $\ln[k_n S_3(n)]$ vs $\ln k_n$ for the cases $q=1.5$ and $q=2.5$, together with the case $q=2$ already considered. Two phenomena are outstanding. First, we observe that, the larger the aspect ratio q, the stronger the oscillations in the structure functions. Second, for $q=1.5$ when there are practically no oscillations, we observe an inertial-range behavior of $S_3(n)\propto k_n^{-\zeta_3}$, with $\zeta_3=1.16\pm 0.04$. There is thus a sig-

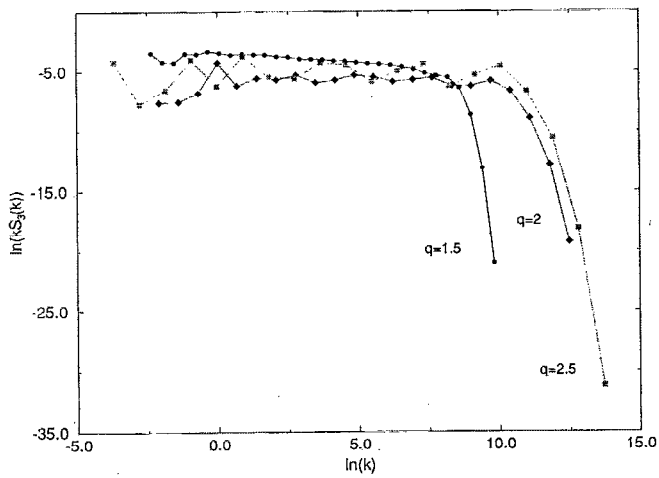

FIG. 4. Third-order structure function $S_3(n)$ multiplied by k_n, vs k_n in log–log scales for three values of the ratio q of successive shell wave numbers. Circles: $q=1.5$, diamonds: $q=2$, squares: $q=2.5$. Notice that oscillations increase dramatically with q and that for $q=1.5$ a clear deviation from a flat scaling is detectable.

nificant discrepancy from the value one, suggested by a loose application of the (analog of the) four-fifth law.

Such discrepancies are not consistent with the usual multifractal model of Parisi and Frisch.[7] We cannot completely rule out the possibility that there is actually no discrepancy in the leading term but only in a subdominant correction. The latter cannot be predicted by standard multifractal phenomenology.

Anyway, it is of interest to look for similar discrepancies in experimental turbulence data. Instead of the usual third-order structure function based on the third moment of the longitudinal velocity increment $v(x+l)-v(x)$, one could try measuring

$$S_3'(l)=\langle [v(x+l)-v(x)]^2[v(x)-v(x-l)]\rangle, \qquad (14)$$

for which there is no "four-fifth law" prediction.

ACKNOWLEDGMENTS

We have benefitted from discussions with S. Gama, M. Hénon, M. H. Jensen, E. Léveque, K. Ohkitani, G. Paladin, Z. S. She, A. Vulpiani, and M. Yamada.

This work was supported by Grants from the European Community (ERBCHRXCT920001) and from DRET (91/112). L.B. was supported by a "Henri Poincaré" fellowship (Centre National de la Recherche Scientifique and Conseil Général des Alpes Maritimes). D.P. was supported by a fellowship from the *Fondation des Treilles.*

[1] F. Anselmet, Y. Gagne, E. J. Hopfinger, and R. A. Antonia, "High order velocity structure functions in turbulent shear flows," J. Fluid Mech. **140**, 63 (1984).

[2] E. B. Gledzer, "System of hydrodynamic type admitting two quadratic integrals of motion," Sov. Phys. Dokl. **18**, 216 (1973).

[3] V. N. Desnyansky and E. A. Novikov, "Evolution of turbulence spectra to self-similar regime," Izv. Akad. Nauk SSSR Fiz. Atmos. Okeana **10**, 127 (1974).

[4] M. Yamada and K. Ohkitani, "Lyapunov spectrum of a chaotic model of three-dimensional turbulence," J. Phys. Soc. Jpn. **56**, 4210 (1987).

[5] K. Ohkitani and M. Yamada, "Temporal intermittency in the energy cascade process and local Lyapunov analysis in fully developed turbulence," Prog. Theor. Phys. **81**, 329 (1989).

[6] M. H. Jensen, G. Paladin, and A. Vulpiani, "Intermittency in a cascade model for three dimensional turbulence," Phys. Rev. A **43**, 798 (1991).

[7] G. Parisi and U. Frisch, "On the singularity structure of fully developed turbulence" in *Turbulence and Predictability in Geophysical Fluid Dynamics*, Proceedings of the International School of Physics "E. Fermi," 1983, Varenna, Italy, edited by M. Ghil, R. Benzi, and G. Parisi (North-Holland, Amsterdam, 1985), p. 84.

[8] U. Frisch, Z. S. She, and O. Thual, "Viscoelastic behavior of cellular solutions to the Kuramoto-Sivashinky model," J. Fluid Mech. **168**, 221 (1986).

[9] G. Paladin and A. Vulpiani, "Degrees of freedom of turbulence," Phys. Rev. A **35**, 1971 (1987).

[10] U. Frisch and M. Vergassola, "A prediction of the multifractal model: the intermediate dissipation range," Europhys. Lett. **15**, 439 (1991).

[11] R. Benzi, L. Biferale, and G. Parisi, "On intermittency in a cascade model for turbulence," Phys. D **65**, 163 (1993).

[12] E. Leveque (private communication, 1993).

[13] L. A. Smith, J. D. Fournier, and E. A. Spiegel, "Lacunarity and intermittency in fluid turbulence," Phys. Lett. A **114**, 465 (1986).